AIAA SPACE 2012 Conference & Exposition
11 - 13 September 2012, Pasadena, California

AIAA 2012-5237

Mission Comparison of Hall Effect and Gridded Ion Thrusters Utilizing Various Propellant Options

Timothy Kokan[1]
Pratt & Whitney Rocketdyne, Huntsville, Alabama, 35806

C. Russell Joyner II[2]
Pratt & Whitney Rocketdyne, West Palm Beach, Florida, 33410

A mission comparison of solar electric propulsion vehicles with Hall effect and gridded ion thrusters utilizing bismuth, xenon, and krypton propellant options is presented. Three example missions are examined: (1) geosynchronous transfer orbit to geostationary orbit, (2) high Earth orbit to the near Earth asteroid 2008 EA9, and (3) high Earth orbit to Mars orbit at the Mars moon Phobos. Trades of power level and specific impulse are performed for each mission, recommended power level and specific impulse ranges are provided, and recommendations for potential future work are provided.

Nomenclature

HEO	=	high Earth orbit
Isp	=	specific impulse
GEO	=	geostationary orbit
GMAT	=	General Mission Analysis Tool
GTO	=	geosynchronous transfer orbit
MER	=	mass estimating relationship
NEA	=	near Earth asteroid
PPU	=	power processing unit
SECKSPOT	=	Solar Electric Control Knob Setting Program by Optimal Trajectories
SEP	=	solar electric propulsion
SOI	=	sphere of influence
TOF	=	time of flight
VARITOP	=	Variational Calculus Trajectory Optimization Program

I. Introduction

HISTORICALLY electric propulsion systems, both fielded and in study, have focused primarily on xenon, and to a lesser extent, krypton, as propellants of choice. The focus on xenon has typically been due to its reasonable ionization energy, high atomic mass, and relative ease of storage and flow measuring[1]. However, xenon's rarity, and corresponding high cost, creates a potential need for alternative propellant options.

This study examines the use of bismuth and krypton as potential propellant alternatives to xenon. The impacts of propellant choice on the overall solar electric propulsion (SEP) vehicle design and example SEP missions comparing bismuth, krypton, and xenon propellant options are provided.

II. Background

Xenon is typically the propellant of choice for most electric propulsion applications. Unfortunately xenon production is a highly expensive process that involves extraction from air as a byproduct of the separation of nitrogen and oxygen. In addition to electric propulsion, xenon is used with increasing demand in a wide variety of other applications including lighting, television displays, lasers, and anesthetics[2]. This increasing demand combined with an expensive production process dependent upon the demand for nitrogen and oxygen (xenon production is a

[1] Staff Engineer, Systems Analysis, 555 Discovery Drive, AIAA Senior Member.
[2] Fellow, Space Systems & Mission Analysis, P.O. Box 109600 MS712-67, AIAA Associate Fellow.

byproduct of industrial nitrogen and oxygen production through the fractional distillation of air) results in the potential for a continued rapid increase in xenon cost going forward. This potential increase in xenon cost provides motivation for examining alternative electric propulsion propellants.

Two such alternatives are krypton and bismuth. Krypton is appealing due to the fact that it has been used previously in electric propulsion applications, is a noble gas like xenon with similar handling and feed system characteristics, and is thus well understood from an overall vehicle system point of view. Additionally, its costs are significantly lower than those of xenon. A drawback of krypton is that it typically has lower thruster efficiency, relative to xenon due to its lower atomic mass and higher ionization energy. Bismuth is appealing due to its relative abundance and ease of production and potentially high thruster efficiency. Bismuth, however, unlike the noble gases xenon and krypton, is a solid metal at standard conditions. These factors result in the need to utilize alternative storage and feed system designs for bismuth relative to its noble gas counterparts. Several methods have been either studied or used for bismuth feed systems but they are typically more complex and less developmentally mature than corresponding noble gas feed systems[3].

Table 1 provides thermodynamic, physical, and approximate cost information for xenon, krypton, and bismuth[4]. Atomic mass and energy requirements associated with heating, melting, vaporization, dissociation, and ionization together affect thruster efficiency. A propellant with a higher atomic mass and lower required energy input needed for the above physical transitions has the potential for higher thruster efficiency. Bismuth's combination of high atomic mass, low ionization energy, and manageable phase transition energies makes it an attractive potential alternative to xenon. An engineering challenge with bismuth is its relatively high melting and boiling points as compared to xenon and krypton. These high melting and boiling points make for a more challenging feed system design likely requiring investment in the maturity of bismuth feed systems. The abundance of both krypton and bismuth relative to xenon translates into lower propellant costs for krypton and substantially lower propellant costs for bismuth.

Table 1. Selected Properties of Xenon, Krypton, and Bismuth.

	Xenon	Krypton	Bismuth
Atomic Mass, amu	131.29	83.8	208.98
Heating, Melting, Vaporization, and Dissociation Energy, eV	0.0	0.0	3.0
Ionization Energy, eV	12.12	14.0	7.29
Melting Point, C	-111.9	-157.2	271.3
Boiling Point, C	-108.1	-152.3	1559
Abundance	0.087 ppm in air	1.14 ppm in air	Abundant solid material
Approximate Cost, $/kg	~1,200	~330	~20

Figure 1 shows the percentage of total power that is required for ionization for different propellant options as a function of specific impulse (Isp)[1]. Krypton, due to its combination of high ionization energy and relatively low atomic mass, requires the highest percentage of total power for ionization of all propellants shown. Cesium and bismuth have the lowest percentage due to their combination of low ionization energy and relatively high atomic mass. Xenon is in between the two extremes. This figure helps to illustrate why bismuth is viewed as an attractive potential alternative to xenon. The low percentage of power required for ionization translates to potentially high thruster efficiency.

Taken together, the combination of potentially high thruster efficiency and low propellant costs make bismuth an attractive alternative to xenon. Similarly, krypton's low propellant cost relative to xenon makes it an attractive alternative as the cost of xenon propellant continues to rise.

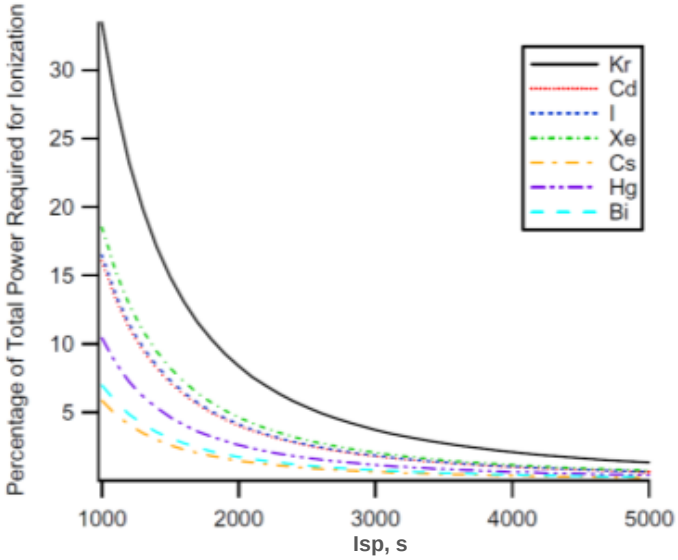

Figure 1. Ionization Power Requirements for Different Propellants.

III. Multidisciplinary Design Process

All spacecraft trades were performed by examining a variety of conceptual vehicle design disciplines utilizing several vehicle design tools. Table 2 provides a list of disciplines examined and the corresponding tools or sources for those disciplines.

Table 2. Conceptual Vehicle Design Disciplines Utilized.

Discipline	Tool / Source
Trajectory	SECKSPOT, VARITOP, GMAT, Copernicus
Weights and Sizing	Excel Mass Estimating Relationships
Thruster Performance	Engine test, flight data
Tool Integration	ModelCenter

Low thrust in-space trajectory analysis was performed using four primary tools: (1) the Solar Electric Control Knob Setting Program by Optimal Trajectories (SECKSPOT)[5], (2) the Variational Calculus Trajectory Optimization Program (VARITOP)[6], (3) the General Mission Analysis Tool (GMAT)[7], and (4) Copernicus Trajectory Design and Optimization System[8]. SECKSPOT and VARITOP were used for mission trades and parametric studies while GMAT and Copernicus were used for higher fidelity mission point designs and trajectory analysis verification.

Weights and sizing analysis was performed using subsystem mass estimating relationships (MERs) derived primarily from published NASA Jet Propulsion Lab MERs[9,10,11]. MERs for primary structures and mechanisms, main propulsion (including thrusters and gimbals, power processing units (PPU), main propellant tanks, main propellant feed system, and cabling), attitude control system/reaction control system, primary power (including batteries, power distribution, power regulation and control, solar array, and spacecraft harnesses), avionics (including guidance, navigation, and control, command and data handling, and communication), and environmental control (including tank insulation/tank heat dissipation and radiators) were used in estimating vehicle dry mass. Additionally, allowances for main propellant reserves and residuals and payload adapter mass were included.

Thruster performance was determined using thruster efficiency curves as a function of delivered Isp generated using the general approach presented by Auweter-Kurtz in 2003[12]. These thruster efficiency curves were anchored to engine test data for gridded ion and Hall effect thrusters utilizing xenon, bismuth, and krypton.

The above tools were linked together using Phoenix Integration's ModelCenter® frameworks environment[13]. As a result of the ability to automate the linking of tools and design variables, ModelCenter enables rapid vehicle convergence, parametric studies, optimization, and visualization. Figure 2 is a screenshot of ModelCenter.

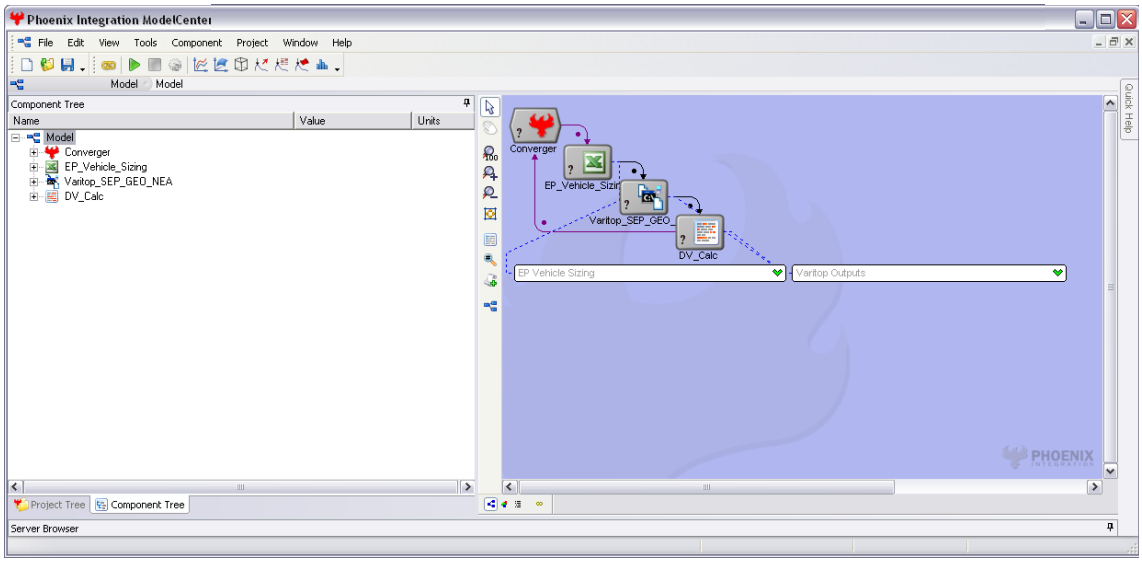

Figure 2. Multidisciplinary Conceptual Vehicle Design Process Utilizing ModelCenter.

IV. Mission Analysis Results

Three primary missions were examined as part of this study: (1) geosynchronous transfer orbit (GTO) to geostationary orbit (GEO), (2) high Earth orbit (HEO) to the near Earth asteroid (NEA) 2008 EA9, and (3) HEO to Mars orbit at the Mars moon Phobos. Sweeps of vehicle system power and delivered Isp were performed and results including vehicle gross mass, required propulsive ΔV, and total time of flight (TOF) were analyzed.

For all three missions, assumptions were made for PPU efficiency, ΔV margin, reserves and residuals percentage, payload adapter mass, and dry mass growth allowance. A PPU efficiency of 95% was assumed for all trades as a representative state-of-the-art PPU efficiency[9]. A ΔV margin of 5% is assumed for all propulsive ΔV's to account for trajectory modeling uncertainties. Propellant reserves and residuals were assumed to be 1% of the total usable propellant to account for a limited amount of reserve propellant plus any unusable residual propellants left in the tanks and feedlines after all propulsive ΔV's are performed. A standard payload adapter mass of 2.5% of the payload mass is assumed to account for structures and mechanisms needed to mount the payload to the spacecraft. Additionally, a 30% stage dry mass growth allowance is added to the subsystem dry masses to account for subsystem MER uncertainty.

A. Mission #1: GTO to GEO

Mission #1 is a GTO to GEO trajectory approximating a GEO satellite launch profile utilizing SEP for orbit raising and final orbital insertion. Figure 3 is a GMAT visualization of this type of low thrust GTO to GEO trajectory. A payload of 1,000 kg was assumed for this mission. A system power of 9 kWe was assumed in order to approximate a Boeing 702SP-type satellite[14]. Two active thrusters were assumed with two redundant thrusters included. SECKSPOT was used for the trajectory analysis.

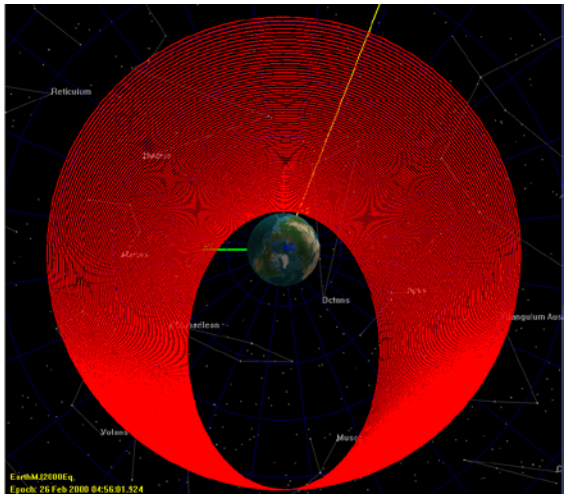

Figure 3. GTO to GEO Low Thrust Trajectory.

Figure 4 is a plot of total vehicle gross mass (including payload) as a function of thruster delivered Isp for gridded ion and Hall effect thrusters utilizing xenon, krypton, and bismuth propellants. The vehicle gross mass is constant across the different thruster and propellant options for a given Isp due to the nature of the MERs used for the vehicle subsystems. In an actual system, one would expect to see some differences in the subsystem masses across the different thruster and propellant options. Figure 4 instead provides a general vehicle sizing trend and can be used to

determine thruster Isp ranges for a given desired vehicle gross mass, perhaps for informing launch vehicle choice. As can be seen in Figure 4, increased thruster Isp translates non-linearly into decreased vehicle gross mass. For reference, the Boeing 702SP spacecraft has a gross mass of approximately 1,820 kg at an Isp of 3,800 s[15,16].

Figure 5 is a plot of time of flight from GTO to GEO as a function of thruster delivered Isp. Over the range of Isp's examined, Hall effect thrusters consistently had shorter time of flights for all propellant options compared to their gridded ion counterparts. This is due to the fact that Hall effect thrusters have superior thruster efficiency over the range of Isp's examined as compared to gridded ion thrusters. Up to an Isp of approximately 2,500 s, Hall-bismuth thrusters provided the shortest time of flight. Above 2,500 s, Hall-xenon thrusters begin to provide a slightly shorter time of flight. If time of flight is most important for GTO to GEO mission transfers, which it often is for commercial GEO satellites whose owners desire to get to their operational orbit as soon as possible so that they can begin operating and producing revenue, then Hall effect thrusters with relatively low Isp's are preferable.

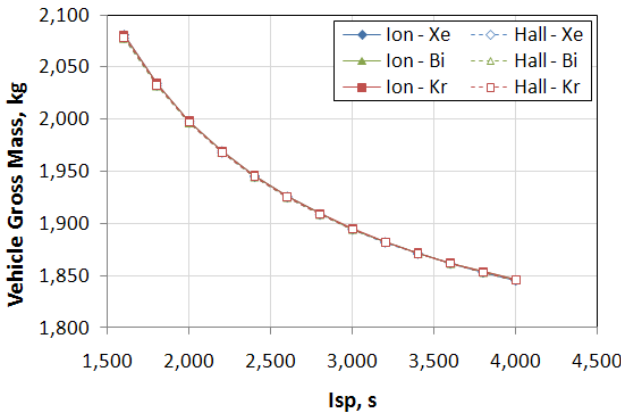

Figure 4. Vehicle Gross Mass vs. Isp.

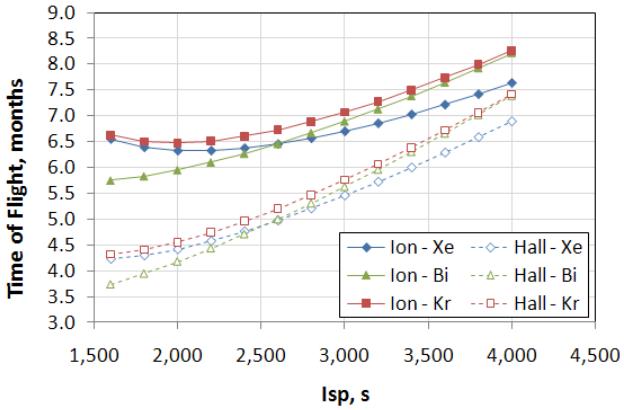

Figure 5. Vehicle GTO to GEO time of flight vs. Isp.

For instance, a thruster such as that used on the Boeing 702SP with an Isp of 3,800 s translates to a time of flight of 6.6 months for a Hall-xenon thruster and 7.4 months for a gridded ion-xenon thruster. This time of flight can be reduced substantially by utilizing a Hall effect thruster in the Isp range of 2,000-2,500 s. Over this range, the time of flights range from 4.2 months for Hall-bismuth at 2,000 s Isp to 5.1 months for Hall-krypton at 2,500 s Isp.

Using typical values for number of transponders per satellite (48 according to the 2011 FAA Commercial Space Transportation Forecast[17]), yearly revenue per transponder ($1.7M according to French[18]), and transponder usage rate (85% according to the 2011 FAA Commercial Space Transportation Forecast[17]), this decrease in time of flight of 2-3 months translates into average increased initial operating revenue per satellite of $12M to $17M.

B. Mission #2: HEO to NEA

Mission #2 is a HEO to NEA mission from a 5,000 km circular Earth orbit to the NEA 2008 EA9. Figure 6 is a depiction of this low thrust trajectory. Like Mission #1, a payload of 1,000 kg was assumed for this mission. System power level and Isp were varied while vehicle gross mass, required ΔV, and time of flight were analyzed.

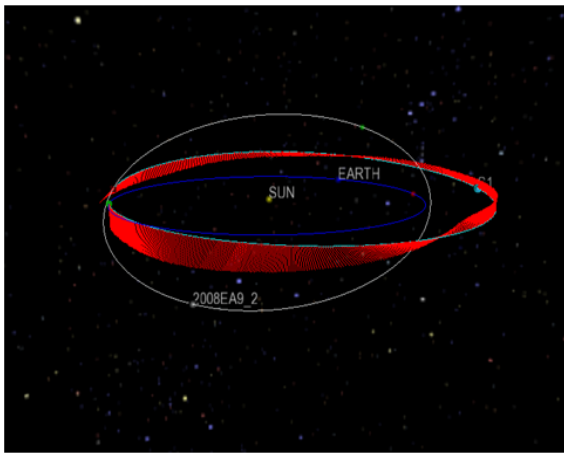

Figure 6. HEO to NEA Low Thrust Trajectory.

Based upon the results from Mission #1, a multi-propellant architecture was chosen for Mission #2. A Hall-bismuth thruster with an Isp of 2,500 s was chosen for the Earth departure spiral from HEO to the Earth's sphere of influence (SOI). A Hall effect thruster was chosen due to its superior efficiency as compared to gridded ion thrusters at lower Isp values desired for Earth spiral trajectories. In terms of propellant options for the Hall effect thruster, bismuth and xenon have very similar thruster efficiencies at an Isp of 2,500 s and both are superior to krypton. Bismuth was chosen over xenon due to bismuth's significantly lower propellant cost. A Hall-xenon thruster was chosen for the remaining portions of the trajectory from Earth SOI to orbital insertion near the target NEA due to its superior efficiency at

higher Isp values desired for heliocentric trajectories. Two active thrusters were assumed with two redundant thrusters included. Each thruster was assumed to be able to switch between bismuth and xenon propellants. Departure from Earth SOI was set for May 30, 2018. VARITOP was used for the trajectory analysis.

Two trades were performed as part of Mission #2. Trade #1 examined varying system power from 2-19 kWe. For this trade, the Hall-bismuth Earth departure spiral Isp was held constant at 2,500 s. The Hall-xenon heliocentric and target NEA orbital insertion Isp was held constant at 3,000 s. Trade #2 examined varying the Hall-xenon Isp from 1,500-4,000 s. Similar to Trade #1, the Hall-bismuth Earth departure spiral Isp was held constant at 2,500 s. Additionally, the system power level was held constant at 9 kWe.

1. Mission #2, Trade #1: System Power Trade

Figure 7, Figure 8, and Figure 9 provide plots of total vehicle gross mass (including payload), required ΔV, and time of flight respectively. Vehicle gross mass is linear with system power ranging from approximately 2,000 kg at 2 kWe to approximately 3,500 kg at 19 kWe.

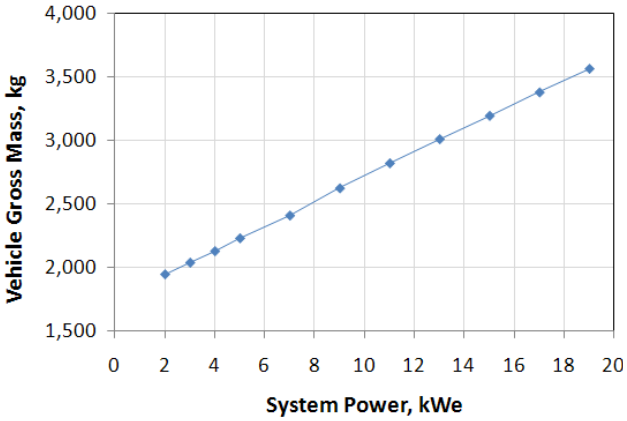

Figure 7. Vehicle Gross Mass vs. System Power.

In terms of ΔV's, the Earth departure spiral and NEA arrival spiral ΔV's decrease slightly with increasing system power. This is due to the fact that as system power increases, at constant Isp, this results in increasing thrust. Increasing thrust during the Earth departure spiral phase results in fewer spiral passes, shorter times of flight, and lower overall gravity losses.

Conversely, the heliocentric ΔV increases with increasing system power. In this case the higher thrust at the higher system power levels results in shorter, straighter, more direct heliocentric trajectories from the Earth departure location to the NEA arrival location. This shorter, straighter heliocentric trajectory results in higher heliocentric ΔV gravity losses as the velocity vector of the vehicle is less normal to the vehicle's local gravity vector.

In terms of time of flight, as expected the departure spiral, heliocentric, and arrival spiral times all decrease with increasing system power. This is because the higher thrust afforded by the higher system power allows for quicker accelerations and decelerations. The total time of flight decreases rapidly from a system power level of 2 kWe to approximately 5 kWe. The knee of the time of flight curve occurs between 5-9 kWe with the curve leveling off past 9 kWe.

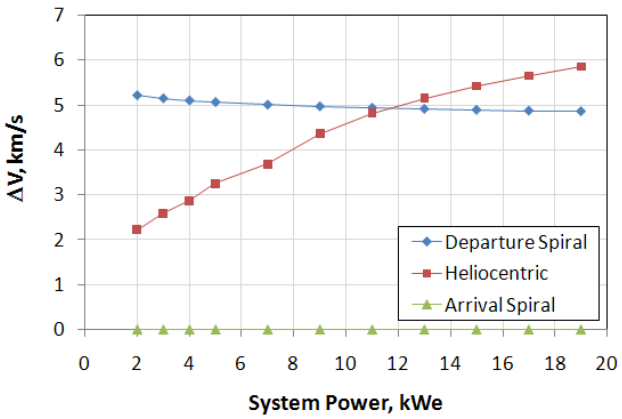

Figure 8. Vehicle ΔV vs. System Power.

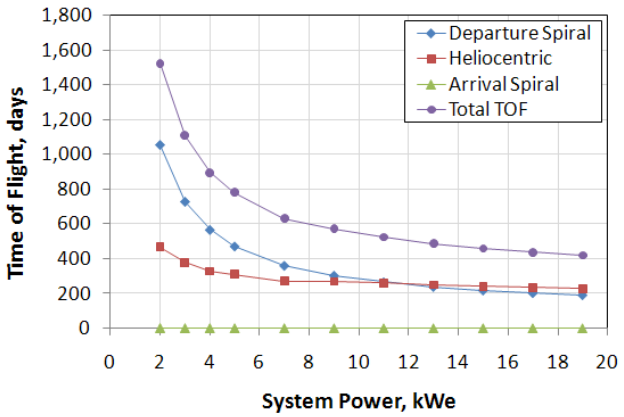

Figure 9. Vehicle Time of Flight vs. System Power.

2. Mission #2, Trade #2: Hall-Xenon Isp Trade

Figure 10, Figure 11, and Figure 12 provide plots of total vehicle gross mass (including payload), required ΔV, and time of flight respectively. Vehicle gross mass decreases non-linearly with increasing heliocentric Isp.

In terms of ΔV's, the Earth departure spiral and NEA arrival spiral ΔV's decrease very slightly, but are nearly constant with increasing heliocentric Isp. Heliocentric ΔV decreases more substantially with increasing heliocentric Isp. Increasing heliocentric Isp translates to decreasing heliocentric thrust with system power held constant. This decreasing heliocentric thrust results in a longer heliocentric trajectory whose velocity vector is more normal to the vehicle's local gravity vector translating into less heliocentric ΔV gravity losses.

In terms of time of flight, heliocentric time of flight increases slightly with increasing heliocentric Isp while departure and arrival spiral time of flights decrease more rapidly. Departure and arrival spiral time of flights decrease as heliocentric Isp increases because the overall vehicle gross mass decreases. This results in a higher departure and arrival spiral vehicle thrust-to-weight. This higher vehicle thrust-to-weight translates into higher vehicle acceleration which results in shorter time of flights. The total time of flight value decreases rapidly from heliocentric Isp values between 1,500-2,500 s with the knee of the curve between 2,000-3,000 s.

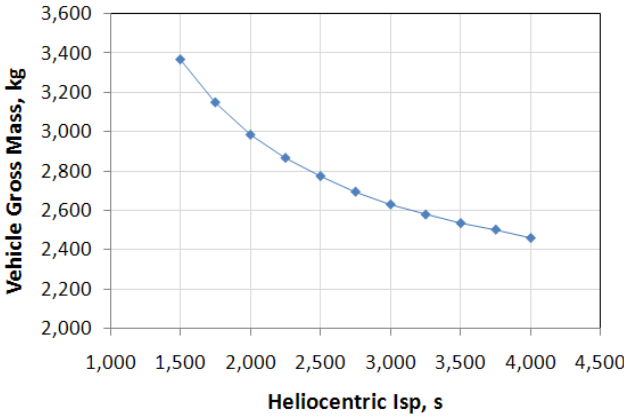

Figure 10. Vehicle Gross Mass vs. Heliocentric Isp.

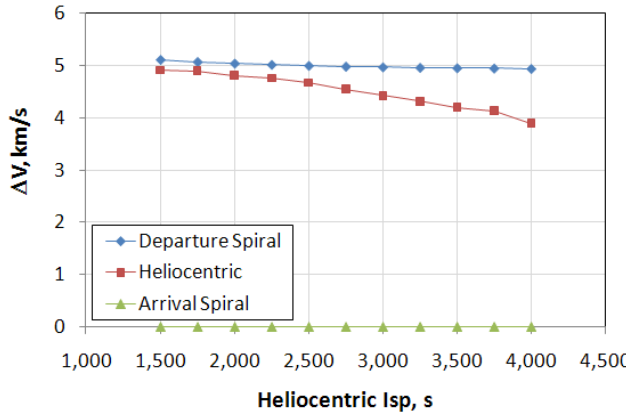

Figure 11. Vehicle ΔV vs. Heliocentric Isp.

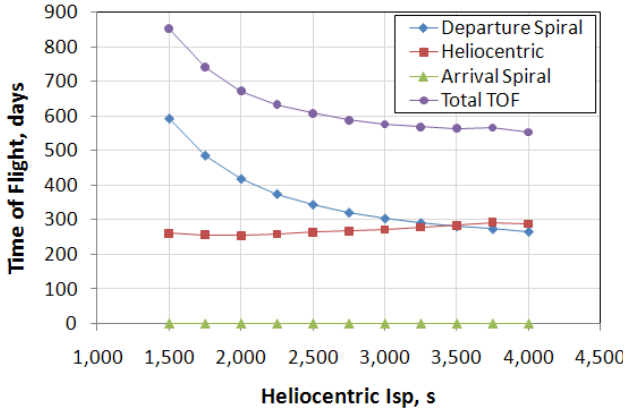

Figure 12. Vehicle Time of Flight vs. Heliocentric Isp.

Figure 13 and Figure 14 are summary contour plots of the vehicle gross mass and time of flight respectively for Mission #2. They show the overall relationship between the Trade #1 and Trade #2 results illustrating the system power and heliocentric Isp design space. These contour plots show the interaction between Isp and system power for both vehicle gross mass and time of flight.

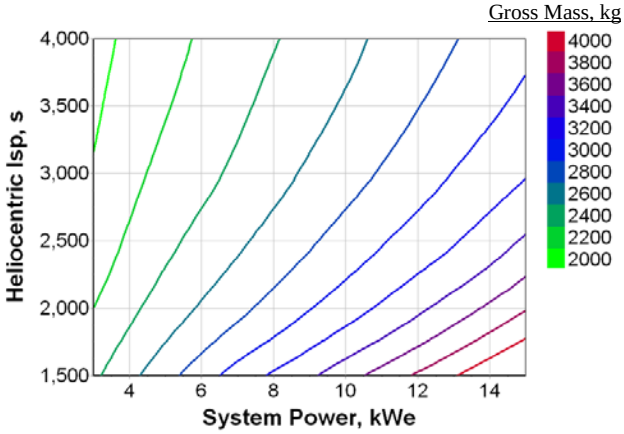

Figure 13. Vehicle Gross Mass vs. Heliocentric Isp and System Power.

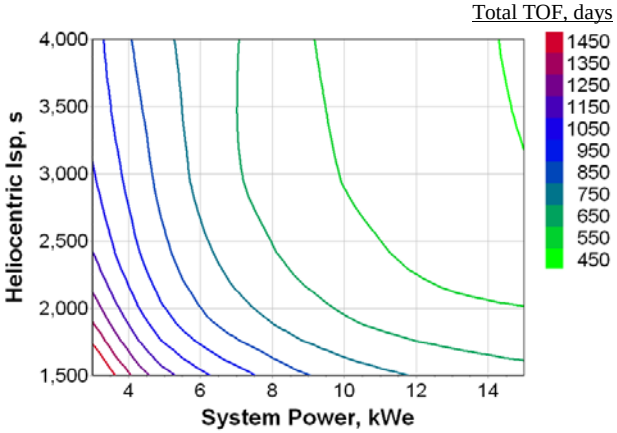

Figure 14. Vehicle Time of Flight vs. Heliocentric Isp and System Power.

As can be seen in Figure 13, at higher system power levels, vehicle gross mass is more sensitive to heliocentric Isp than at lower power levels. This is due to the fact that the total ΔV is higher at higher power levels due to the increase in heliocentric ΔV (Figure 8). This ΔV increase translates into higher mass ratios and larger propellant loads. At lower heliocentric Isp values, vehicle gross mass is more sensitive to system power than at lower heliocentric Isp values.

As can be seen in Figure 14, at higher system power levels, time of flight is less sensitive to heliocentric Isp than at lower power levels. This is due to the fact that at higher power levels vehicle thrust-to-weight is higher for a given Isp. This results in less sensitivity to Isp (and resulting thrust) changes. At higher heliocentric Isp values, time of flight is less sensitive to system power than a lower heliocentric Isp values.

C. Mission #3: HEO to Mars/Phobos

Mission #3 is a HEO to Mars/Phobos mission from a 5,000 km circular Earth orbit to Mars orbit at the Mars moon Phobos. Figure 15 is a depiction of this low thrust trajectory. For this mission a payload of 4,000 kg was assumed. This payload was chosen in order to have the highest payload value possible while still being able to launch the spacecraft into the 5,000 km circular orbit with an Atlas V or Delta IV launch vehicle. Like Mission #2, system power level and Isp were varied while vehicle gross mass, required ΔV, and time of flight were analyzed.

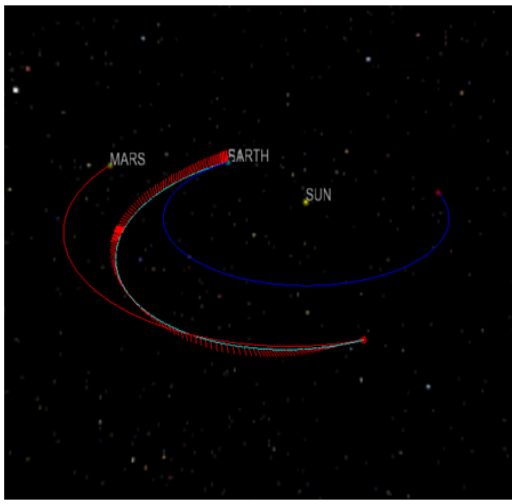

Figure 15. HEO to Mars/Phobos Low Thrust Trajectory.

Similar to Mission #2, a multi-propellant architecture was chosen for Mission #3. The Earth departure spiral and heliocentric portions use the same thruster-propellant combination as Mission #2: Hall-bismuth for Earth departure and Hall-xenon for heliocentric. Unique to Mission #3, the Hall-bismuth thruster is used for the Mars arrival spiral. This change from the Mission #2 plan of simply using the Hall-xenon thruster for both the heliocentric and arrival burns was made due to the fact that the arrival burn for Mission #3 is into a deeper gravity well Mars orbit. This results in a larger benefit for going to the lower cost bismuth propellant for the arrival burn. Three active thrusters were assumed with two redundant thrusters included. Each thruster was assumed to be able to switch between bismuth and xenon propellants. Departure from Earth SOI was set for May 31, 2028. VARITOP was used for the trajectory analysis.

Two trades were performed as part of Mission #3. Trade #1 examined varying system power from 24-50 kWe. For this trade, the Hall-bismuth Earth departure and Mars arrival spiral Isp's were held constant at 2,500 s. The Hall-xenon heliocentric Isp was held constant at 3,000 s. Trade #2 examined varying the Hall-xenon Isp from 1,500-4,000 s. Similar to Trade #1, the Hall-bismuth Earth departure and Mars arrival spiral Isp's were held constant at 2,500 s. Additionally, the system power level was held constant at 30 kWe.

1. *Mission #3, Trade #1: System Power Trade*

Figure 16, Figure 17, and Figure 18 provide plots of total vehicle gross mass (including payload), required ΔV, and time of flight respectively. Vehicle gross mass is linear with system power ranging from approximately 9,300 kg at 24 kWe to approximately 12,000 kg at 50 kWe.

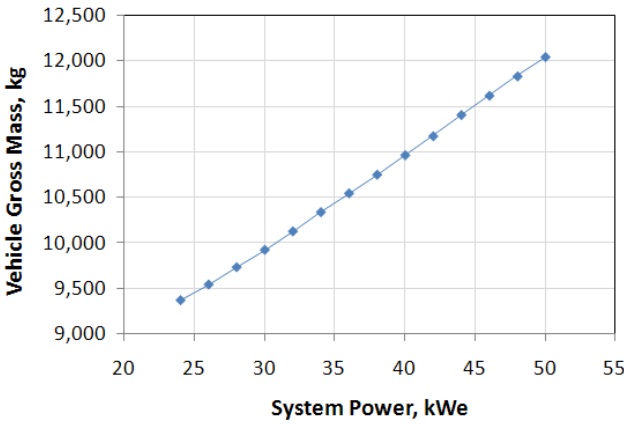

Figure 16. Vehicle Gross Mass vs. System.

ΔV and time of flight trends are similar to those found in Mission #2, Trade #1 with the exception that the arrival spiral ΔV for Mission #3 is higher than in Mission #2 due to the fact that Mission #3 is going to the deeper gravity well Mars orbit rather than the heliocentric orbit near NEA 2008 EA9. Earth departure spiral and Mars arrival spiral ΔV's decrease slightly with increasing system power while the heliocentric ΔV increases with increasing system power.

Earth departure spiral, heliocentric, and Mars arrival spiral time of flights all decrease with increasing system power. Similarly to Mission #2, Trade #1, the sensitivity of time of flight to system power decreases with increasing system power.

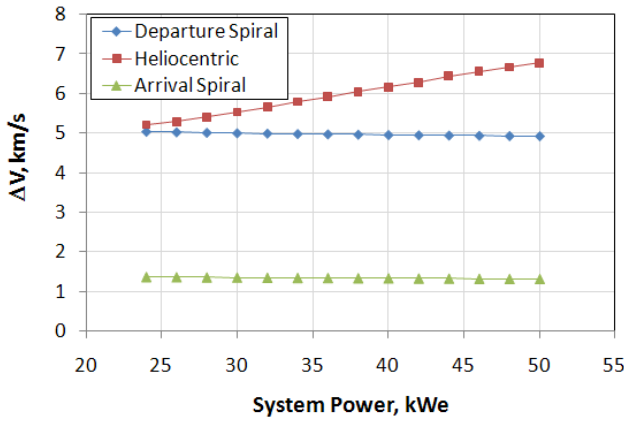

Figure 17. Vehicle ΔV vs. System Power.

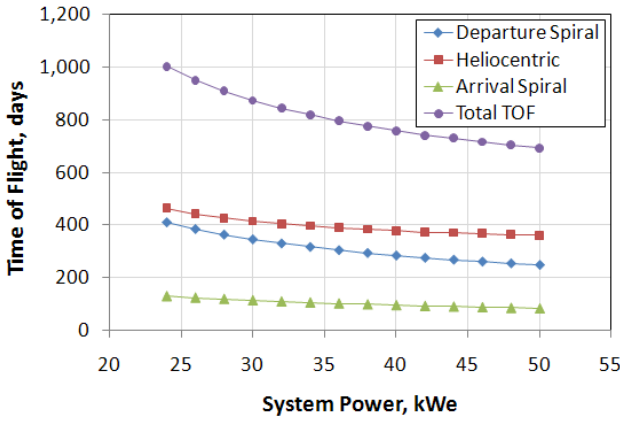

Figure 18. Vehicle Time of Flight vs. System Power.

2. Mission #3, Trade #2: Hall-Xenon Isp Trade

Figure 19, Figure 20, and Figure 21 provide plots of total vehicle gross mass (including payload), required ΔV, and time of flight respectively. Vehicle gross mass decreases non-linearly with increasing heliocentric Isp.

The ΔV and time of flight trends are similar to Mission #2, Trade #2, with the exception being that the Mars arrival spiral ΔV and time of flight is higher than the corresponding values for the NEA arrival case. Earth departure spiral and Mars arrival spiral ΔV's decrease very slightly with increasing heliocentric Isp while heliocentric ΔV decreases more rapidly.

Heliocentric time of flight increases slightly with increasing heliocentric Isp while Earth departure and Mars arrival spiral time of flights decrease. The combination of these effects results in a minimum time of flight at a heliocentric Isp of 3,500 s while the time of flight is fairly insensitive to heliocentric Isp in the range from 3,000-4,000 s.

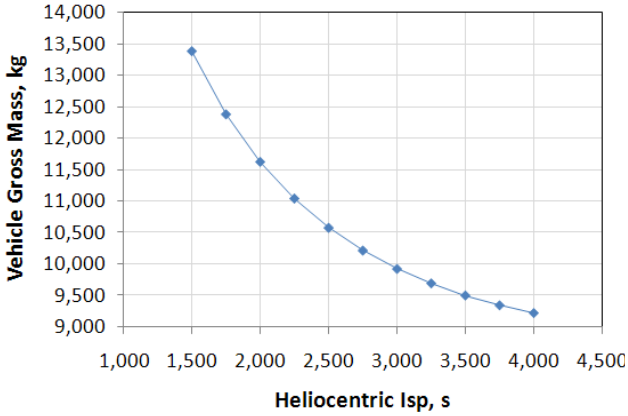

Figure 19. Vehicle Gross Mass vs. Heliocentric Isp.

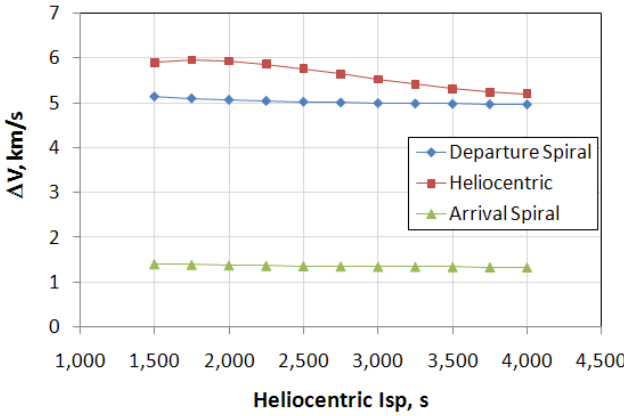

Figure 20. Vehicle ΔV vs. Heliocentric Isp.

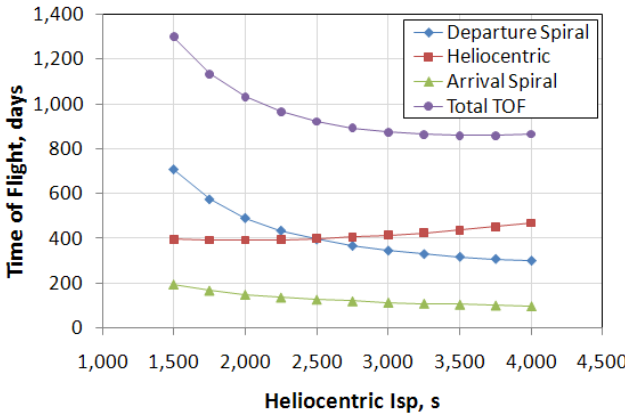

Figure 21. Vehicle Time of Flight vs. Heliocentric Isp.

Figure 22 and Figure 23 are summary contour plots of the vehicle gross mass and time of flight respectively for Mission #3. Similar to Mission #2, these contour plots show the overall relationship between the Trade #1 and Trade #2 results illustrating the interaction between system power and heliocentric Isp. These contour plot trends show similar interactions between system power and heliocentric Isp as those found in Mission #2.

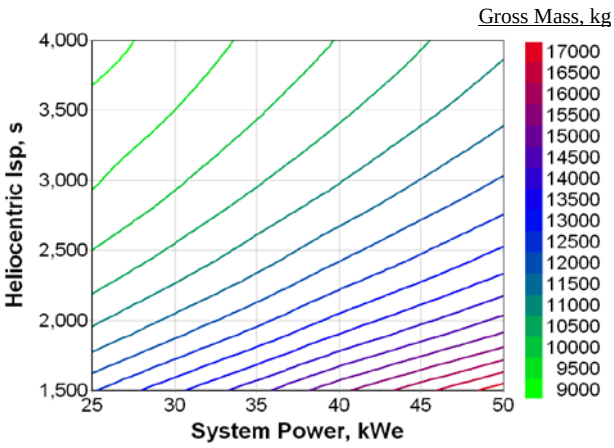

Figure 22. Vehicle Gross Mass vs. Heliocentric Isp and System Power.

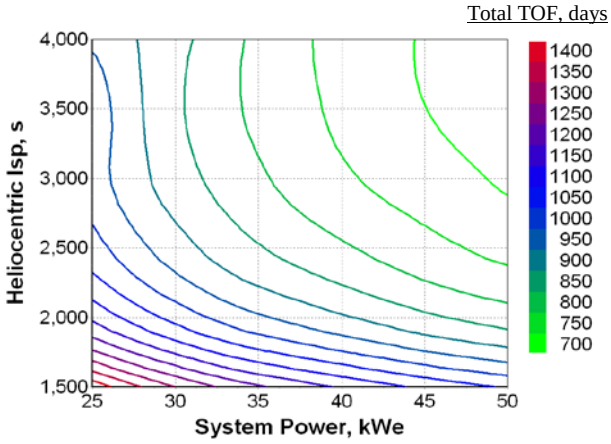

Figure 23. Vehicle Time of Flight vs. Heliocentric Isp and System Power.

These contour plots can be used to determine heliocentric Isp and system power level target values in order to stay within launch vehicle payload targets. In order to provide a robust launch vehicle payload margin, a reasonable power level with a higher heliocentric Isp in the 3,000-4,000 s range where time of flight is at a minimum looks to make the most sense. The Atlas V 552 has a payload capability of 10,500 kg[19] to the 5,000 km circular Earth orbit while the Delta IV Heavy has a payload capability of 13,900 kg[20] to this orbit.

Using Figure 22, one can determine the combination of heliocentric Isp and system power level such that the vehicle gross mass stays under the launch vehicle payload capability of both the Atlas V 552 and Delta IV Heavy with some margin. If the target vehicle gross mass is 10,000 kg (500 kg margin with respect to the Atlas V 552), then one can see that at a heliocentric Isp of 2,500 s, the system power level should be no higher than 25 kWe. Following the 10,000 kg line on Figure 22, at a heliocentric Isp of 4,000 s, the system power level can be up to 40 kWe.

Using Figure 23, the 2,500 s / 25 kWe point has a total time of flight of approximately 1,025 days while the 4,000 s / 40 kWe point has a total time of flight of approximately 730 days. In order to minimize total time of flight while still keeping the vehicle gross mass at or below 10,000 kg, a reasonable range of heliocentric Isp would be 3,500-4,000 s and a reasonable range of system power level would be 35-40 kWe.

V. Conclusions

A mission comparison of SEP vehicles with Hall effect and gridded ion thrusters utilizing bismuth, xenon, and krypton propellant options was performed for three different missions: (1) GTO to GEO, (2) HEO to NEA 2008 EA9, and (3) HEO to Mars/Phobos.

A. Results Summary

The results indicate that for GTO to GEO missions, Hall effect thrusters can produce significantly shorter time of flight values than gridded ion thrusters due to their superior efficiency over the range of Isp values examined. Furthermore, Hall-bismuth thrusters can produce shorter time of flights than Hall-xenon thrusters for Isp values below 2,500 s. Above 2,500 s, Hall-xenon thrusters produce shorter time of flights. Hall-krypton thrusters consistently produced the longest time of flights of all Hall effect thruster options over the range of Isp values examined. Additionally, a comparison to the Boeing 702SP spacecraft was discussed and it was shown that by switching from the 702SP's gridded ion xenon thruster at an Isp of 3,800 s to either a Hall-bismuth or Hall-xenon thruster at an Isp of 2,000-2,500 s, the time of flight could be decreased by 2-3 months. This resulting reduction in time of flight could translate into additional initial operating revenue of $12M to 17M per satellite.

For the HEO to NEA mission analyzed, a multi-propellant architecture was chosen based upon the results from the GTO to GEO mission analysis. Hall-bismuth was chosen for the Earth departure spiral due to the superior efficiency of Hall effect thrusters at the lower Isp values desired for Earth spiral trajectories. Bismuth was chosen over xenon due to bismuth's significantly lower propellant cost with approximately the same overall thruster efficiency. Hall-xenon was chosen for the remaining portions of the trajectory from Earth SOI to NEA arrival due to its superior efficiency at the higher Isp values desired for heliocentric trajectories.

Results indicate that a system power level of at least 9 kWe is desirable due to the time of flight increasing rapidly at system power levels below 9 kWe. Above 9 kWe, the time of flight decreases more slowly and begins to level off while vehicle gross mass continues to increase linearly. For heliocentric Isp, results indicate that an Isp greater than 2,500 s is desirable as both vehicle gross mass and time of flight increase rapidly at Isp values below that point. If there is a desire to have spacecraft commonality between the GTO to GEO and HEO to NEA missions, then a power level of approximately 9 kWe with an Isp of approximately 2,500 s would provide a good compromise between GTO to GEO and HEO to NEA vehicle gross masses and time of flights.

For the HEO to Mars/Phobos mission analyzed, a similar multi-propellant architecture to the HEO to NEA mission was chosen. Hall-bismuth was chosen for the Earth departure spiral, Hall-xenon for the heliocentric burn, with an additional propellant transition to Hall-bismuth for the Mars arrival spiral. The transition to Hall-bismuth for the Mars arrival spiral was added due to the larger arrival ΔV into Mars orbit as compared to the NEA arrival ΔV. Hall-bismuth has an advantage over Hall-xenon for these types of large ΔV's into and out of moderate to large gravity fields due to its comparable thruster efficiency to Hall-xenon at the lower Isp values desired with these types of ΔV's combined with its significantly lower propellant cost (which is only partially offset by the need for multiple propellant feed systems).

Results indicate that a system power level in the range of 35-40 kWe and a heliocentric Isp level in the range of 3,500-4,000 s is desirable in order to allow for the ability for the spacecraft to be launched on either an Atlas V 552 or a Delta IV Heavy. System power levels greater than the 35-40 kWe range increase the vehicle gross mass and drive towards eliminating the Atlas V 552 as a launch vehicle option.

B. Future Work

Several areas of future work would be useful in furthering these propellant and mission studies. A detailed examination of bismuth feed systems, potential heating/melting/vaporization techniques, and subsequent impacts on the overall feed system and vehicle design would be useful in better understanding the next steps needed in bismuth electric propulsion development. A more detailed examination of the cost impacts of propellant choice for the various missions would also be important in helping to better differentiate between the propellant options. Finally, a development roadmap showing the steps required and development phasing to go from low power, low Isp thrusters for GTO to GEO missions, transitioning to the HEO to NEA missions, and then on to higher power, higher Isp thrusters for HEO to Mars/Phobos missions would be useful in better understanding the timing and phasing required for development. This development roadmap should include the examination of technology maturity and how it could be inserted into these design architectures.

References

[1]Kieckhafer, A., and King, L.B., "Energetics of Propellant Options for High-Power Hall Thrusters," *Space Nuclear Conference 2005*, American Nuclear Society, San Diego, California, 2005.

[2]Parissenti, G. et al., "Non Conventional Propellants for Electric Propulsion Applications," *Space Propulsion 2010*, AAAF-ESA-CNES, San Sebastian, Spain, Paper No. 1841086, 2010.

[3]Polzin, K.A., Markusic, T.E., and Stanojev, B.J., "Integrated Liquid Bismuth Propellant Feed System," *42nd AIAA Joint Propulsion Conference and Exhibit*, Sacramento, California, AIAA Paper 2006-4636, 2006.

[4]Scharfe, D.B., "Alternative Hall Thruster Propellants Krypton and Bismuth: Simulated Performance and Characterization," Ph.D. Dissertation, Department of Mechanical Engineering, Stanford Univ., Stanford, California, 2009.

[5]Sackett, L.L, Malchow, H.L., and Edelbaum, T.N., "Solar Electric Geocentric Transfer With Attitude Constraints: Analysis," NASA CR-134927, 1975.

[6]Sauer, Jr., C.G., "Users Guide To The Operation Of Varitop: A General Purpose, Low-Thrust, Trajectory Optimization Program," NASA Jet Propulsion Laboratory, Pasadena, California, 1998.

[7]GMAT, General Mission Analysis Tool, Software Package, Ver. R2011a, NASA Goddard Space Flight Center, Greenbelt, Maryland, 2011.

[8]Copernicus Trajectory Design and Optimization Software, NASA Johnson Space Center, Houston, Texas, 2011.

[9]Brophy, J.R., Gershman, R., Strange, N., and Landau, D., "300-kW Solar Electric Propulsion System Configuration for Human Exploration of Near-Earth Asteroids," *47th AIAA Joint Propulsion Conference and Exhibit*, San Diego, California, AIAA Paper 2011-5514, 2011.

[10]Brophy, J.R., Gershman, R., Landau, D., Polk, J., Porter, C., and Yeomans, D., "Asteroid Return Mission Feasibility Study," *47th AIAA Joint Propulsion Conference and Exhibit*, San Diego, California, AIAA Paper 2011-5665, 2011.

[11]Hofer, R.R., and Randolph, T.M., "Mass and Cost Model for Selecting Thruster Size in Electric Propulsion Systems," *47th AIAA Joint Propulsion Conference and Exhibit*, San Diego, California, AIAA Paper 2011-5518, 2011.

[12]Auweter-Kurtz, M., and Kurtz, H., "Optimization of Electric Thrusters for Primary Propulsion Based on the Rocket Equation," *AIAA Journal of Propulsion and Power*, Vol. 19, No. 3, May-June 2003.

[13]PHX ModelCenter, Software Package, Ver. 9.0, Phoenix Integration, Inc., Wayne, PA.

[14]"Boeing 702SP Satellite," The Boeing Company, URL: http://www.boeing.com/defense-space/space/bss/factsheets/702/702SP.html [cited 17 July, 2012].

[15]Mecham, M., "Boeing Adds Its Smallest 702 Satellite," Aviation Week, URL: http://www.aviationweek.com/Article.aspx?id=/article-xml/asd_03_14_2012_p03-02-435949.xml [cited 17 July, 2012]

[16]"Xenon Ion Propulsion Center," The Boeing Company, URL: http://www.boeing.com/defense-space/space/bss/factsheets/xips/xips.html [cited 17 July, 2012]

[17]"2011 Commercial Space Transportation Forecasts," Federal Aviation Administration, HD-111393.INDD, May 2011.

[18]French, P., "$$$ Per Transponder," Northern Sky Research, URL: http://www.nsr.com/news-resources/the-bottom-line/-per-transponder/ [cited 17 July, 2012].

[19]"Atlas Launch System Mission Planner's Guide – Revision 10a," Lockheed Martin Corporation, Denver, Colorado, January 2007.

[20]"Delta IV Payload Planners Guide," United Launch Alliance, Littleton, Colorado, September 2007.